GJR Publication
OPEN ACCESS
Global Journal of Research in Engineering & Computer Sciences
ISSN: 2583-2727 (Online)
Volume 05| Issue 04 | July-Aug. | 2025
Journal homepage: https://gjrpublication.com/gjrecs/
Research Article

Repercussions and Difficulties of Feedback Linearization-Based Optimal Control of a Doubly-Fed Induction Generator

*Sadiq Abubakar Ahmed [1], Abba Lawan Isah [2], Amanatu Kabir [3], Musa Dan-azumi Mohammed [4], Ahmad Muhammad Ahmad [5], Munirah Abdullahi Said [6]

[1]Department of Mathematical Sciences, Bayero University Kano (BUK), Nigeria.
[2]Department of Civil Engineering, Nigerian Defence Academy (NDA), Kaduna, Nigeria.
[3]Department of Computer Science, School of Technology, Kano State Polytechnic, Nigeria.
[4,5,6] Kano State Institute for Information Technology, Kura, Nigeria.

DOI: 10.5281/zenodo.16739653 **Submission Date:** 01 July 2025 | **Published Date:** 04 Aug. 2025

***Corresponding author:** Sadiq Abubakar Ahmed*
Department of Mathematical Sciences, Bayero University Kano (BUK), Nigeria.

Abstract
A full-order nonlinear model of a wind turbine doubly-fed induction generator (DFIG-WT) that takes stator dynamics into account has been examined in this work. To regulate the rotor speed of a doubly-fed induction generator (DFIG) in a wind energy conversion system (WECS), a nonlinear multi-input-multi-output (MIMO) feedback linearization controller has been developed. The device is driven at the ideal rotor speed for maximum power point tracking by selecting the required states. The rotor might not maintain the ideal speed because wind speed is unpredictable. For the rotor-side converter, a model predictive controller (MPC) with output limitations has been developed to guarantee that the rotor maintains its ideal speed at all operating points. Additionally, it increases the rotor speed's transient state. This study discusses the benefits of using feedback linearization (FBL) in conjunction with model predictive control (MPC) for DFIG-based wind turbines. However, there are drawbacks as well, such as increased computational complexity and potential sensitivity to model inaccuracies.

Keywords: *Impacts, DFIG-WT, Maximum Power Point Tracking, Feedback linearization, Model predictive control, Challenges.*

I. Introduction
Power generation from renewable energy is ever growing due to global warming disquiets, hikes in oil prices, and government policies towards clean energy [1-3]. The fastest-growing source of renewable energy is wind power. The power is generated when the wind speed is enough to rotate the blades of the turbine. The mechanical energy of the rotating blades is converted to electricity by a generator. The preferred location of wind farms is offshore sites where the wind is stronger. Offshore wind farms generate sustainable energy in large quantities, contrary to land wind farms [4]. At the moment, the doubly-fed induction generator (DFIG) is predominantly used for offshore applications. The main advantages of DFIG for this application are generating power at low wind speed, generating power at constant frequency and voltage even though the rotor speed is varying, maintaining unity power factor, revamped efficiency, and cost-effectiveness [5-7]. DFIG has both rotor and stator windings. The rotor windings are connected to the grid via back-to-back converters. The back-to-back converters are responsible for regulating both the grid and the rotor currents. Rotor current regulation makes it possible to regulate the active and reactive powers fed to the load from the stators, and this is independent of the rotor speed [8, 9]. The stator windings are directly connected to the grid by means of the tertiary winding of the transformers. The control of DFIG is more complex than that of a traditional induction generator. The operation of DFIG can be drastically affected by the capricious wind speed if there were no control system incorporated into it. Similarly, incessant connection of loads to the electrical system by the consumers of electricity can severely affect the DFIG system without any control [11]. Over the years, many researchers have come up with numerous control techniques to make the DFIG system robust, such as well as be able to handle any undesired disturbance it may

encounter. The most common of such techniques is conventional vector control. It allows separate control of active and reactive power based on the assumptions that the stator flux is constant and the stator resistance is negligible [12, 13]. This method suffers a huge setback under grid fault or when the wind speed is varying. As a result, the stator flux is no longer constant. Furthermore, the dynamics of vector control solely depend on the fine-tuned gains of the proportional-integral (PI) controller. However, selecting such gains to ensure stability under varying load is arduous [14]. Moreover, a PI controller is applied in [15] to control the grid-side converter of DFIG. Further improvement upon this, a fuzzy logic-based controller has been designed in [16] to smoothen the output power oscillation from the grid-side converter. Model Predictive Controller (MPC) can conquer the aforementioned limitation of the PI controller and offer an excellent solution for current, flux, power, and torque control [17]. MPC is easier to design, cost-effective, and has a faster response than a PI controller. Nevertheless, coordinate MPC controllers for rotor-side converters (RSCs) and stator-side converters (SSCs) hardly have any significant improvement on the performance of DFIG [14]. Linear Quadratic Regulator (LQR) based on optimal control has been implemented in [18] for pitch control of DFIG wind turbines. The performance of the LQR pitch control is more effective in comparison to PI pitch control. [19] employed Genetic Algorithm (GA) to obtain optimal matrices. The overall performance of this controller is superior to that in [18]. The aforementioned control techniques are based on the approximated linear model of DFIG near a particular operating point. The controllers give satisfactory performances only near this point. As a result, these controllers are not suitable for DFIG in Wind Energy Conversion Systems (WECS). This is because DFIG is required to operate under variable speed and a wide range of operating points due to capricious wind speed. Therefore, nonlinear control techniques must be employed to cope with the nonlinearities in the system and achieve acceptable wind energy conversion. Nonlinear robust sliding mode control has been successfully applied in [20] to control the grid voltage. However, the chartering effect augments the mechanical wear. The chattering effect can be attenuated by using higher-order sliding mode [21]. Second-order sliding mode, also known as the super-twisting algorithm, has been applied in [22] to attain maximum power point tracking (MPPT). Furthermore, adaptive backstepping control capable of eliminating uncertainties in the system has been described in [23]. Backstepping approach for achieving

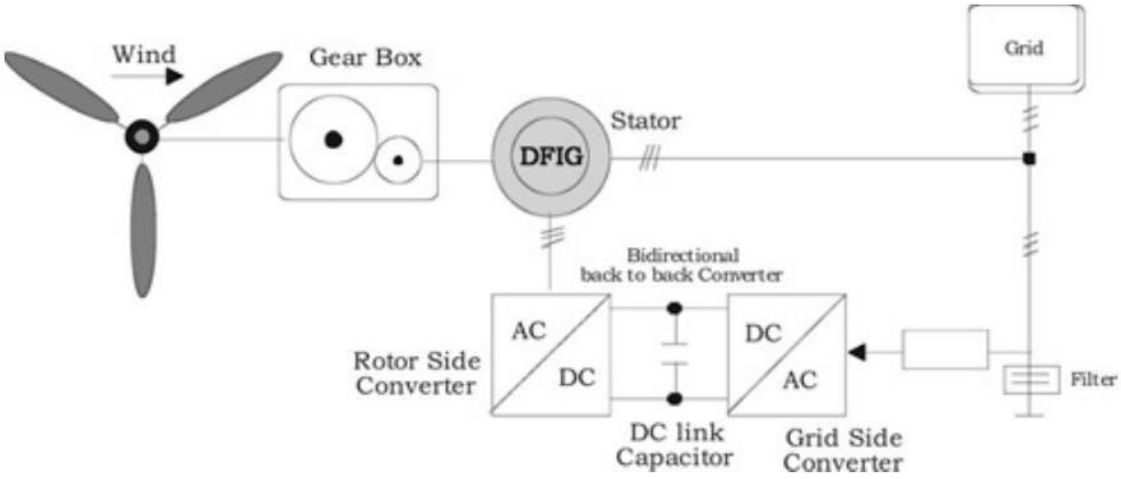

Fig. 1. Wind energy conversion system DFIG [10] reference tracking has been implemented in [23] to control the rotor side converter.

Adaptive feedback linearization together with an observer for estimating model uncertainties was employed to improve the performance of wind turbine DFIG [24]. A decentralized feedback linearization controller has been proposed for wind turbine DFIG using differential geometry to improve the transient stability of the power system [25]. Feedback linearization control for the current loop was used to attain maximum power point tracking in [26]. The aforementioned nonlinear controllers were based on a reduced-order model of DFIG. The stator dynamics were ignored to reduce the order of the model. This greatly reduced the computational complexity and simplified control design at the expense of accuracy. In this paper, the full-order nonlinear model of DFIG together with the stator dynamics has been put into consideration to overcome the limitation of the aforementioned models. Furthermore, four inputs and four outputs of the DFIG are considered for control design, unlike the aforesaid. A feedback linearization controller has been proposed for input-output decoupling of the system to allow coordinated control of the rotor current and stator flux. This allows the speed to be regulated in such a way as to achieve maximum power point tracking. Model Predictive Controller (MPC) with output constraints has been designed for the rotor side to ensure that the rotor retains optimal speed for all operating points. It also improves the transient state of the rotor speed. The paper is organized as follows: In section I, the mathematical model of DFIG-WT has been derived. In section II, the proposed control schemes have been implemented

in section III. The simulation results and the effectiveness of the proposed control schemes have been shown in section IV. The conclusion of the work has been carried out in section V. Also, the impacts and challenges of the feedback linearization-based model Predictive control of rotor speed of DFIG-WT is discussed in this research.

II. Advantages of the Feedback Linearization Based Model Predictive Control of Rotor Speed of DFIG-WT

i. **Handles Nonlinearities:**
FBL transforms the nonlinear DFIG model into a linear one, making it easier to apply MPC, which is typically designed for linear systems. This allows for better control performance in the presence of wind speed variations and other nonlinearities inherent in wind turbines.

ii. **Constraint Handling:**
MPC, with or without FBL, can explicitly handle constraints on rotor speed, currents, and other system variables, leading to more robust and safer operation.

iii. **Performance Improvement:**
Compared to traditional controllers like PI regulators, FBL-based MPC can achieve better performance in terms of tracking speed, stability, and power quality.

iv. **Flexibility:**
FBL-based MPC can be adapted to various wind turbine configurations and operating conditions by adjusting the model and constraints within the MPC framework.

v. **Reduced Computational Complexity (compared to pure nonlinear MPC):**
FBL simplifies the online solution of the complex optimization problem in nonlinear MPC, making it more feasible for real-time implementation.

III. Disadvantages of the Feedback Linearization Based Model Predictive Control of Rotor Speed of DFIG-WT

i. **Model Dependence:**
FBL relies on an accurate mathematical model of the DFIG. Inaccuracies in the model can lead to performance degradation or even instability.

ii. **Increased Computational Burden:**
While FBL reduces the computational burden of nonlinear MPC, it still involves more complex calculations than linear MPC or traditional controllers, potentially requiring more powerful processing units.

iii. **Sensitivity to Parameters:**
The effectiveness of FBL-based MPC can be sensitive to uncertainties in system parameters, requiring careful parameter tuning or robust control design.

iv. **Complexity of Implementation:**
Implementing FBL-based MPC can be more challenging than simpler control strategies due to the need for understanding and implementing the feedback linearization technique and the MPC algorithm.

v. **Potential for Oscillations:**
If not properly tuned, the control loop can exhibit oscillations, especially during transient conditions or when dealing with uncertainties.

vi. **Additional Hardware:**
In some cases, additional hardware like static synchronous compensators (STATCOMs) or dynamic voltage restorers (DVRs) might be needed to improve grid support during faults, adding to the system's complexity and cost [33].

IV. Mathematical Modelling of DFIG

The schematic diagram of the DFIG is depicted in Fig. 1. The full order mathematical model of DFIG-WT in direct and quadrature dq- synchronization frame can be derived as [27, 28]. Application of Kirchhoff's voltage and current laws at all the loops and the nodes of the dq-equivalent circuit diagram [27], the following equations are derived.

$$\frac{d\Psi_{sd}}{dt} = \omega_1 \Psi_{sq} - R_s i_{sd} + u_{sd} \quad (1)$$

$$\frac{d\Psi_{sq}}{dt} = \omega_1 \Psi_{sd} - R_s i_{sq} + u_{sq} \quad (2)$$

$$\frac{d\Psi_{rd}}{dt} = \omega_s \Psi_{rq} - R_r i_{rd} + u_{rd} \quad (3)$$

$$\frac{d\Psi_{rq}}{dt} = \omega_s \Psi_{sd} - R_r i_{rq} + u_{rq} \quad (4)$$

$$\frac{d\omega_r}{dt} = \frac{n_p}{J}(T_e - T_m) \quad (5)$$

$$\Psi_{sd} = L_m i_{rd} + L_s i_{sd} \quad (6)$$

$$\Psi_{sq} = L_m i_{rq} + L_s i_{sq} \quad (7)$$

$$\Psi_{rd} = L_m i_{sd} + L_r i_{rd} \quad (8)$$

$$\Psi_{rq} = L_m i_{sq} + L_r i_{rq} \quad (9)$$

$$T_e = \frac{3L_m n_p}{2L_s}\left(\Psi_{sd} i_{rq} - \Psi_{sq} i_{rd}\right) \quad (9)$$

Where:

u_{sd}, u_{sq}	d-q components of stator voltage
i_{sd}, i_{sq}	d-q components of stator current
Ψ_{sd}, Ψ_{sq}	d-q components of stator flux
u_{rd}, u_{rq}	d-q components of rotor voltage
i_{rd}, i_{rq}	d-q components of rotor current
Ψ_{rd}, Ψ_{rq}	d-q components of rotor flux
R_s, R_r	Rotor and stator resistances respectively
L_m, L_r and L_s	Mutual, rotor and stator inductances respectively
J	Generator rotational inertia
T_e	Electromagnetic torque
n_p	Number of pairs of poles

Further evaluations and transforming the state variables, the dynamic equations can be written in the form

$$\dot{x}_1 = -a_1 x_1 + a_2 x_2 + a_3 x_3 + u_1 \quad (10)$$

$$\dot{x}_2 = -a_2 x_1 - a_1 x_2 + a_3 x_4 + u_2 \quad (11)$$

$$\dot{x}_3 = a_4 x_1 - a_5 x_2 x_5 - a_6 x_3 + a_7 x_4 - a_5 u_1 + a_{10} u_3 \quad (12)$$

$$\dot{x}_4 = a_5 x_1 x_5 + a_4 x_2 - a_7 x_3 - a_6 x_4 - a_5 u_2 + a_{10} u_4 \quad (13)$$

$$\dot{x}_5 = a_8(x_1 x_4 - x_2 x_3) - a_9 \quad (14)$$

$$y_1 = x_1 \quad (14)$$

$$y_2 = x_2 \quad (14)$$

$$y_3 = x_4 \quad (14)$$

$$y_4 = x_5 \quad (14)$$

The nonlinear differential equations can be written in normal form:

$$\begin{cases} \dot{x} = f(x) + g(x)u \\ y = h(x) \end{cases} \tag{15}$$

Where:

$x = [x_1 \quad x_2 \quad x_3 \quad x_4 \quad x_5]^\top = [\Psi_{sd} \quad \Psi_{sq} \quad i_{rd} \quad i_{rq} \quad \omega_r]^\top$

$u = [u_1 \quad u_2 \quad u_3 \quad u_4]^\top = [u_{sd} \quad u_{sq} \quad u_{rd} \quad u_{rq}]^\top$

$y = [h_1(x) \quad h_2(x) \quad h_3(x) \quad h_4(x)]^\top = [x_1 \quad x_2 \quad x_4 \quad x_5]^\top$

$$f(x) = \begin{bmatrix} -a_1x_1 + a_2x_2 + a_3x_3 \\ -a_2x_1 - a_1x_2 + a_3x_4 \\ a_4x_1 - a_5x_2x_5 - a_6x_3 + a_7x_4 \\ a_5x_1x_5 + a_4x_2 - a_7x_3 - a_6x_4 \\ a_8(x_1x_4 - x_2x_3) - a_9 \end{bmatrix}$$

$$g(x) = \begin{bmatrix} 1 & 0 & 0 & 0 \\ 0 & 1 & 0 & 0 \\ -a_5 & 0 & a_{10} & 0 \\ 0 & -a_5 & 0 & a_{10} \\ 0 & 0 & 0 & 0 \end{bmatrix}$$

$a_1 = \frac{R_s}{L_s}$, $a_2 = \omega_1$, $a_3 = \beta R_s$, $a_4 = \frac{\beta R_s}{\alpha L_s}$, $a_5 = \frac{\beta}{\alpha}$, $a_6 = \frac{R_r + \beta^2 R_s}{\alpha}$, $a_7 = \omega_s$, $a_8 = \frac{3L_m n_p^2}{2JL_s}$, $a_9 = \frac{n_p}{J}T_m$, $a_{10} = \frac{1}{\alpha}$, $\alpha = \frac{(L_r L_s - L_m^2)}{L_s}$, $\beta = \frac{L_m}{L_s}$

V. Control Design

In this section, the proposed controller scheme is presented. The objective is to regulate the speed to an optimal value by coordinated control of rotor current and stator flux.

A. Maximum power point tracking

The amount of power a wind turbine can capture from the wind is given by [26]:

$$p = \frac{1}{2}\rho\pi R_{wt}^2 C_p(\lambda, \theta) V_{wind}^3 \tag{16}$$

$$\lambda = \frac{\omega_r R_{wt}}{K_1 V_{wind}} \tag{17}$$

The power coefficient is a function of both pitch angle θ and tip speed ratio λ defined by [27]:

$$C_p(\lambda, \theta) = 0.5176\left(\frac{116}{\lambda_j} - 0.4\theta - 5\right)e^{\frac{-21}{\lambda_j}} + 0.0068\lambda \tag{18}$$

$$\frac{1}{\lambda_j} = \frac{1}{\lambda_j + 0.08\theta} - \frac{0.035}{\beta^3 + 1} \tag{19}$$

Where ρ is air density, R_{wt} is radius of wind turbine, V_{wind} is wind speed, $C_p(\lambda, \theta)$ is power coefficient, θ is pitch angle and λ is tip speed ratio.

Wind turbine can generate maximum power provided that the power coefficient $C_p(\lambda, \theta)$ is maximum for any wind speed within the wide operation region of the turbine. The power coefficient $C_p(\lambda, \theta)$ can be maximized by maintaining optimal value of the tip speed ratio λ_{opt} and fixed pitch angle θ.

$$C_{p\max} = C_p(\lambda_{opt}, \theta) \tag{20}$$

Therefore, the desired optimal speed is given by:

$$\omega_{rd} = \frac{K_1 \lambda_{opt}}{R_{wt}} V_{wind} \tag{21}$$

B. Feedback linearization

the nonlinear MIMO system is decoupled and linearized based on input-output feedback linearization technique. The output of the system, y_k, is differentiated until the input, u_k, ($k = 1,2,3,4$) appears [26].

$$y_k^{r_k} = L_f^{r_k} h_k + \sum_{k=1}^{n} L_{g_k} L_f^{r_k - 1} h_k u_k;\ k = 1,2,3,4 \tag{22}$$

where $y_k^{r_k}$ denotes the $r_k th$-order derivative of y_k. Each y_k has a r_k. The relative degree of the system is the same as the number of states, $(r = 1 + 1 + 1 + 2 = 5 = n)$. The third state is an internal state whose stability is proved in the subsequent section. Evaluating the Lie derivatives in (22) leads to the system of equations expressed in the matrices below.

$$\begin{bmatrix} \dot{y}_1 \\ \dot{y}_2 \\ \dot{y}_3 \\ \ddot{y}_4 \end{bmatrix} = \begin{bmatrix} L_f h_1(x) \\ L_f h_2(x) \\ L_f h_3(x) \\ L_f^2 h_4(x) \end{bmatrix} + \begin{bmatrix} L_{g1} L_f^0 h_1(x) & L_{g2} L_f^0 h_1(x) & L_{g3} L_f^0 h_1(x) & L_{g4} L_f^0 h_1(x) \\ L_{g1} L_f^0 h_2(x) & L_{g2} L_f^0 h_2(x) & L_{g3} L_f^0 h_2(x) & L_{g4} L_f^0 h_2(x) \\ L_{g1} L_f^0 h_3(x) & L_{g2} L_f^0 h_3(x) & L_{g3} L_f^0 h_3(x) & L_{g4} L_f^0 h_3(x) \\ L_{g1} L_f^1 h_4(x) & L_{g2} L_f^1 h_4(x) & L_{g3} L_f ?^1\, h_4(x) & L_{g4} L_f^1 h_4(x) \end{bmatrix} \begin{bmatrix} u_1 \\ u_2 \\ u_3 \\ u_4 \end{bmatrix}$$

$$[\dot{y}_1 \quad \dot{y}_2 \quad \dot{y}_3 \quad \ddot{y}_4]^\top = A(x) + E(x)u$$

$$A(x) = \begin{bmatrix} -a_1 x_1 + a_2 x_2 + a_3 x_3 \\ -a_2 x_1 - a_1 x_2 + a_3 x_4 \\ a_5 x_1 x_5 + a_4 x_2 - a_7 x_3 - a_6 x_4 \\ a_8[(-a_1 - a_6)x_1 x_4 + (a_2 - a_7)(x_2 x_4 + x_1 x_3) \\ +(a_1 + a_6)x_2 x_3 + a_4 x_5 (x_1^2 + x_2^2)] \end{bmatrix}$$

$$E(x) = \begin{bmatrix} 1 & 0 & 0 & 0 \\ 0 & 1 & 0 & 0 \\ 0 & -a_5 & 0 & a_{10} \\ q_1 & q_2 & q_3 & q_4 \end{bmatrix}$$

where $q_1 = 2a_8(x_4 + a_5 x_2), q_2 = -2a_8(x_3 + a_5 x_1)$, $q_3 = -2a_8 a_{10} x_2$, and $q_4 = 2a_8 a_{10} x_1$, and $\mathrm{Det}(E(x)) = 2a_8 x_2 a_{10}^2 \neq 0$. Therefore, $E^{-1}(x)$ exists.

The stabilizing inputs for the input-output feedback linearization are defined by; $v = [v_1 \quad v_2 \quad v_3 \quad v_4]$. The linear decoupling between the input and output variables of the system is realized by the control input given below.

$$u = E^{-1}(x)(-A(x) + v) \tag{23}$$

Where:

$$[\dot{y}_1 \quad \dot{y}_2 \quad \dot{y}_3 \quad \ddot{y}_4]^\top = [v_1 \quad v_2 \quad v_3 \quad v_4]^\top$$

The control objective is to drive the system to point of maximum power required that the defined in the vector, $\eta^d = [\Psi_{sd}^d \quad \Psi_{sq}^d \quad i_{rq}^d \quad w_r^d] = [y_{1d} \quad y_{2d} \quad y_{3d} \quad y_{4d}]$, so that the equilibrium points are shifted to the origin. The error signals are defined as:

$$e = \eta^d - y$$

$$\begin{bmatrix} v_1 \\ v_2 \\ v_3 \\ v_4 \end{bmatrix} = \begin{bmatrix} \dot{y}_{1d} + K_{p1} e_1 + K_{i1} \int e_1 dt \\ \dot{y}_{2d} + K_{p2} e_2 + K_{i2} \int e_2 dt \\ \dot{y}_{3d} + K_{p3} e_3 + K_{i3} \int e_3 dt \\ \ddot{y}_{4d} + K_{p4} e_4 + K_{i4} \int e_4 dt \end{bmatrix}$$

$$\begin{cases} \ddot{e}_1 + K_{p1}\dot{e}_1 + K_{i1} e_1 = 0 \\ \ddot{e}_2 + K_{p2}\dot{e}_2 + K_{i2} e_2 = 0 \\ \ddot{e}_3 + K_{p3}\dot{e}_3 + K_{i3} e_3 = 0 \\ \ddot{e}_4 + K_{p4}\dot{e}_4 + K_{i4} e_4 = 0 \end{cases}$$

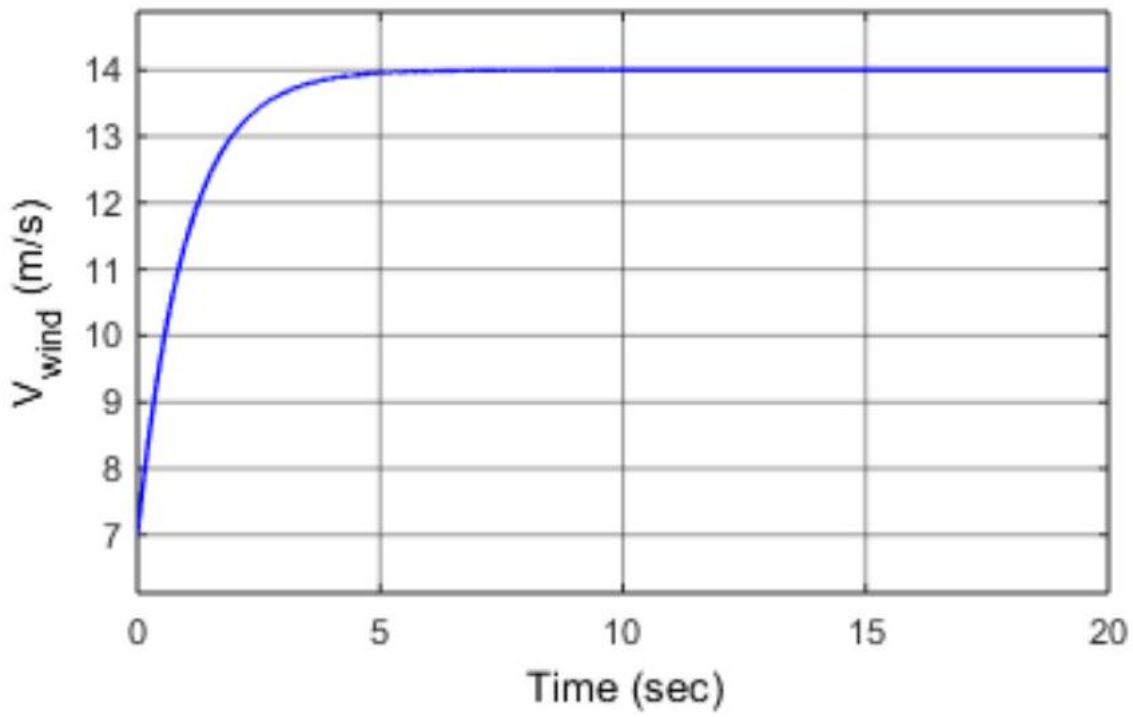

Fig. 2. Wind speed

C. Desired states of the controller

The control targets are the rotor current Ψ and stator flux. The stator oriented-flux frame is aligned with the q-axis. The reference values of the stator flux and its $d-q$ components are given by:

$$\Psi_{sd}^{d} = 0$$
$$\Psi_{sq}^{d} = \Psi^{d} = -\frac{V_s}{\omega_1} = -1$$
$$i_{rq}^{d} = -\frac{\Psi_s^d}{L_m} = -0.34$$

Where $\omega_1 = 1.0\text{pu}$ is synchronous speed, $V_s = 1.0\text{pu}$ is generator rated voltage,

The stabilizing inputs are selected in such a way that the errors converge to zero and the states x_1, x_2, x_4 and x_5 track the reference values $\Psi_{sd}^{d}, \Psi_{sq}^{d}, i_{rq}^{d}$ and w_r^d respectively.

VI. Simulation Result

The performance of the proposed control schemes is evaluated in this section. The parameters of the DFIG-WT are obtained from [32].

The wind speed varies from 7 m/s to 14 m/s and then settles at 14 m/s as shown in Fig. 2. The control objective is to capture maximum power from this wind speed by maximizing the power coefficient and keeping the pitch angle fixed. The maximum power coefficient $(C_{pmax} = 9.0pu)$ is shown in Fig. 3 with the corresponding optimal tip-speed ratio $(\lambda_{\text{opt}} = 0.4569pu)$ at fixed pitch angle $\theta = 1.0$. The turbine will maintain optimal speed and subsequently maximum power as long as the power coefficient remains maximum.

The feedback linearization controller successfully decoupled the rotor and stator dynamics for proper coordinated control. The tuning parameters of the controller are $K_{p1} = 10, K_{i1} = 21, K_{p2} = 4, K_{i2} = 3.5, K_{p3} = 8, K_{i3} = 15, K_{p4} = 22, K_{i4} = 97$.

The d-component and the q-component of the stator flux are shown in Fig. 4 and Fig. 5, respectively. It can be seen that the components of the stator flux have tracked their respective desired values.

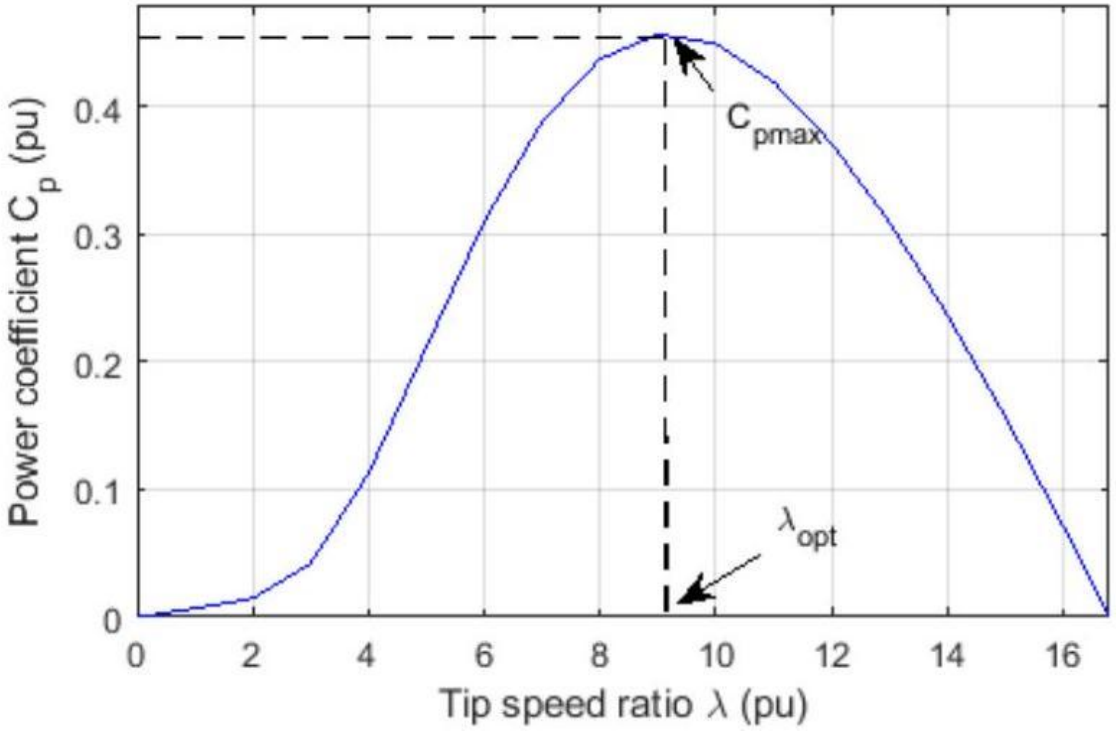

Fig. 3. Power coefficient vs tip-speed ratio

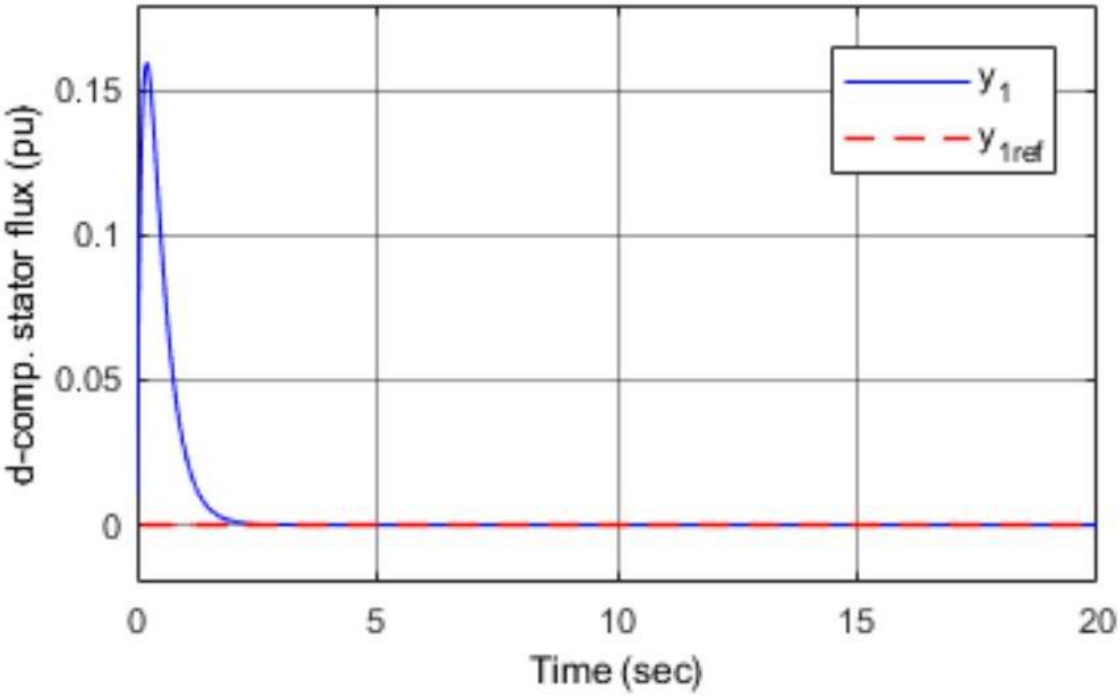

Fig. 4. d-component of stator flux

The q-component of rotor current (y_3) shown in Fig. 6. The speed can be regulated to the optimal speed for the maximum active power generation as shown in Fig. 7.

The tracking errors of the maximum power points converge to zero as shown in Fig. 8.

The control inputs to the DFIG-WT that decouple and ensure the maximum power generation are shown in Fig. 9.

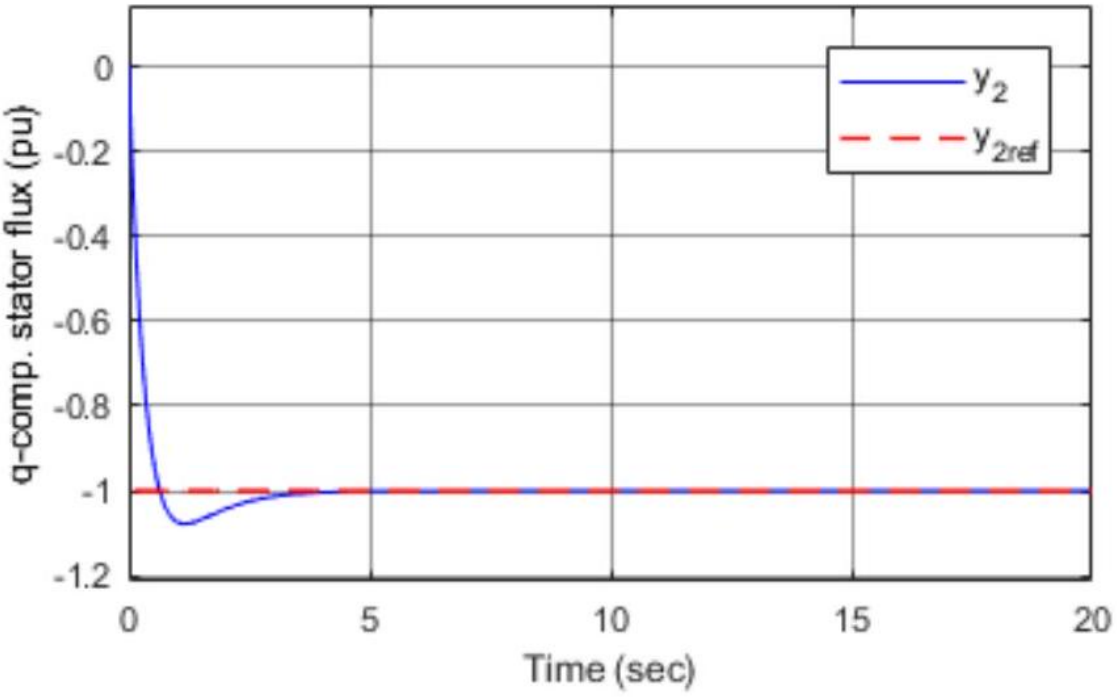

Fig. 5. d-component of stator flux

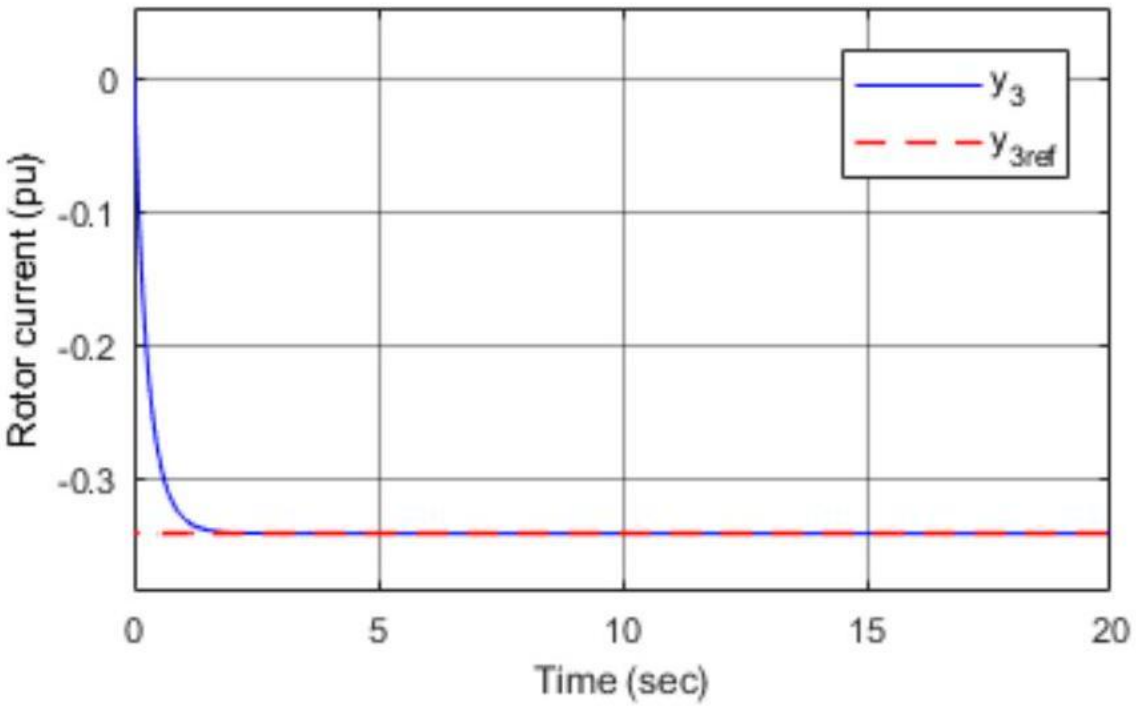

Fig. 6. q-component of rotor current

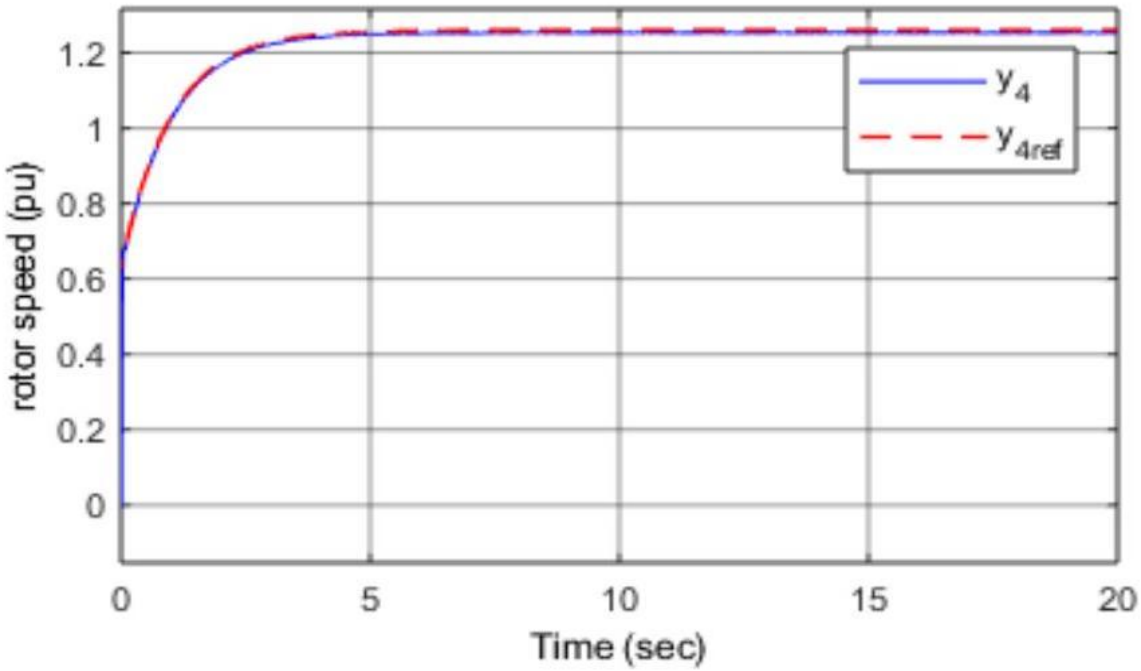

Fig. 7. Optimal rotor speed tracking

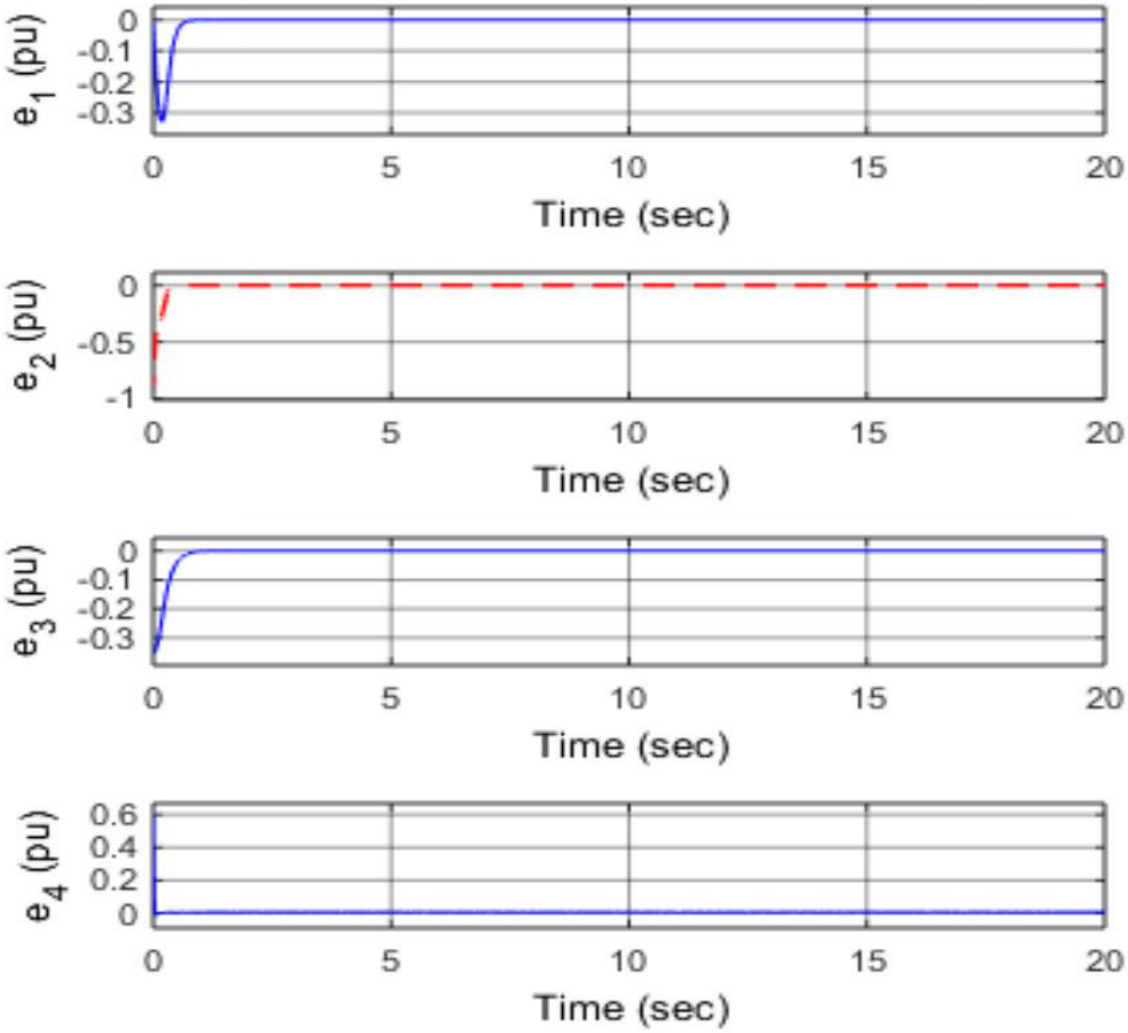

Fig. 8. Tracking errors

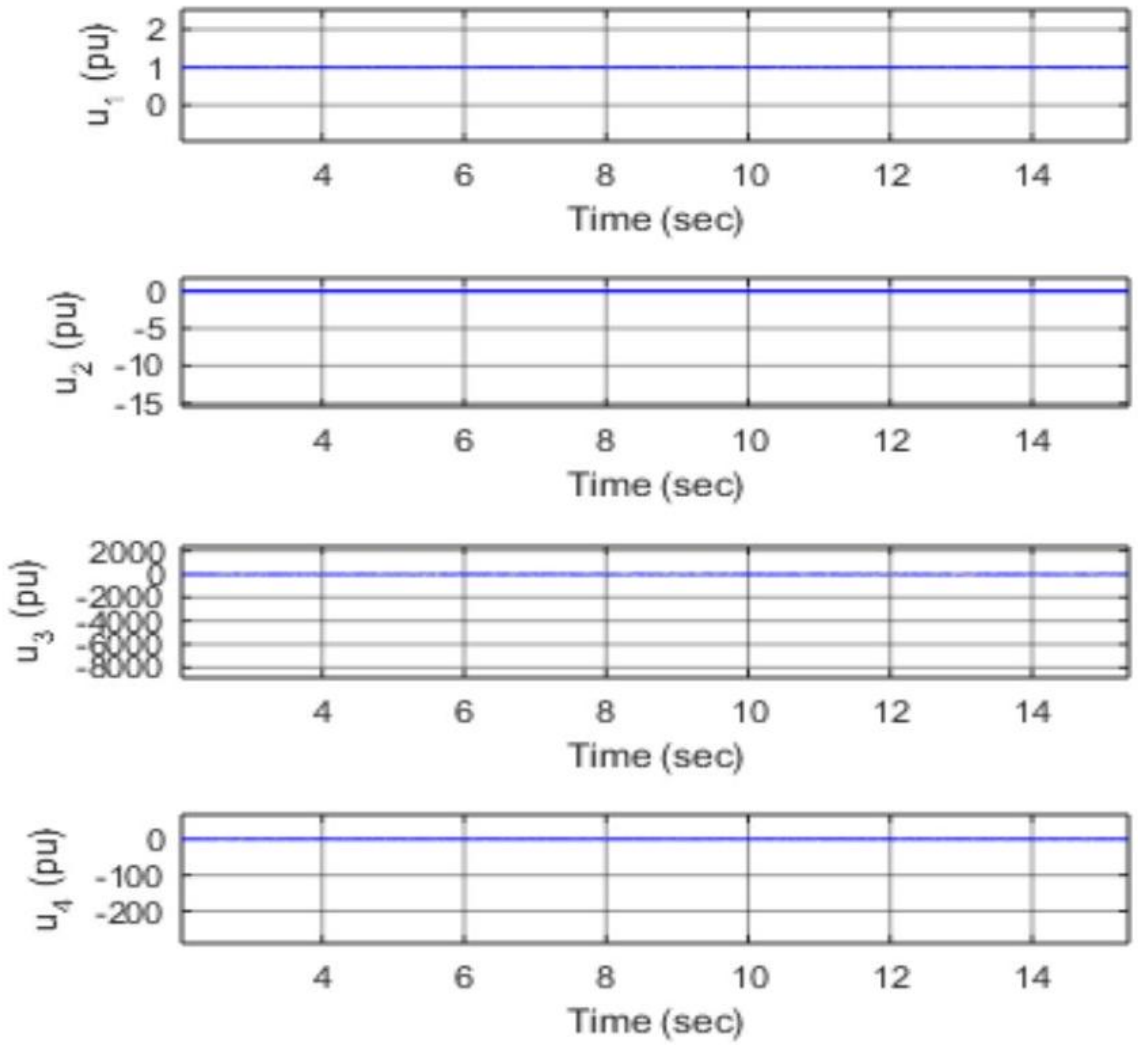

Fig. 9. Control inputs to the DFIG-WT

VII. Conclusion

The DFIG-WT system has been decoupled and linearized using a feedback linearization controller. In order to control the rotor speed to an ideal level, the rotor current and stator flux have been synchronized. The wind turbine can harness the most power from the wind at this speed. However, there is some overshoot in the rotor speed, and tracking the ideal rotor speed for MPPT takes time [34].

References

1. Maaruf, M., & Khalid, M. (2021). Global sliding-mode control with fractional order terms for the robust optimal operation of a hybrid renewable microgrid with battery energy storage. *Electronics, 11*(1), 88. https://doi.org/10.3390/electronics11010088
2. Pena, R., Clare, J. C., & Asher, G. M. (1996). Doubly fed induction generator using back-to-back PWM converters and its application to variable speed wind-energy generation. *IEE Proceedings - Electric Power Applications, 143*(3), 231–241. https://doi.org/10.1049/ip-epa:19960329
3. Cardenas, R., Pena, R., Alepuz, S., & Asher, G. (2013). Overview of control systems for the operation of DFIGs in wind energy applications. *IEEE Transactions on Industrial Electronics, 60*(7), 2776–2798. https://doi.org/10.1109/TIE.2012.2209702
4. Maaruf, M., Khan, K. A., & Khalid, M. (2022). Robust control for optimized islanded and grid-connected operation of solar/wind/battery hybrid energy. *Sustainability, 14*(9), 5673. https://doi.org/10.3390/su14095673
5. Iacchetti, M. F., Marques, G. D., & Perini, R. (2015). A scheme for the power control in a DFIG connected to a DC bus via a diode rectifier. *IEEE Transactions on Power Electronics, 30*(3), 1286–1296. https://doi.org/10.1109/TPEL.2014.2327584

6. (2018). A review of design consideration for Doubly Fed Induction Generator based wind energy system. *Electric Power Systems Research, 160*, 128–141. https://doi.org/10.1016/j.epsr.2018.03.004
7. Maaruf, M., Shafiullah, M., Al-Awami, A. T., & Al-Ismail, F. S. (2021). Adaptive nonsingular fast terminal sliding mode control for maximum power point tracking of a WECS-PMSG. *Sustainability, 13*(23), 13427. https://doi.org/10.3390/su132313427
8. Pena, R., Clare, J. C., & Asher, G. M. (1996). A doubly fed induction generator using back-to-back PWM converters supplying an isolated load from a variable speed wind turbine. *IEE Proceedings - Electric Power Applications, 143*(5), 380–387. https://doi.org/10.1049/ip-epa:19960521
9. [Duplicate of reference 3]
10. Tazil, M., Kumar, V., Bansal, R. C., Kong, S., Dong, Z. Y., Freitas, W., & Mathur, H. D. (2010). Three-phase doubly fed induction generators: An overview. *IET Electric Power Applications, 4*(2), 75–89. https://doi.org/10.1049/iet-epa.2009.0063
11. Maaruf, M., El Ferik, S., & Mahmoud, M. S. (2020). Integral sliding mode control with power exponential reaching law for DFIG. In *2020 17th International Multi-Conference on Systems, Signals and Devices (SSD)* (pp. 1122–1127). IEEE. https://doi.org/10.1109/SSD49366.2020.9364173
12. Yang, B., Jiang, L., Wang, L., Yao, W., & Wu, Q. H. (2016). Nonlinear maximum power point tracking control and modal analysis of DFIG based wind turbine. *International Journal of Electrical Power & Energy Systems, 74*, 429–436. https://doi.org/10.1016/j.ijepes.2015.06.017
13. Marques, G. D., & Iacchetti, M. F. (2019). DFIG topologies for DC networks: A review on control and design features. *IEEE Transactions on Power Electronics, 34*(2), 1299–1316. https://doi.org/10.1109/TPEL.2018.2837506
14. Yan, S., Zhang, A., Zhang, H., Wang, J., & Cai, B. (2018). An optimum design for a DC-based DFIG system by regulating gearbox ratio. *IEEE Transactions on Energy Conversion, 33*(1), 223–231. https://doi.org/10.1109/TEC.2017.2743041
15. Maaruf, M., Khan, K. A., & Khalid, M. (2021). Integrated power management and nonlinear-control for hybrid renewable microgrid. In *2021 IEEE Green Technologies Conference (GreenTech)* (pp. 176–180). IEEE. https://doi.org/10.1109/GreenTech48523.2021.00039
16. Meo, S., Zohoori, A., & Vahedi, A. (2016). Optimal design of permanent magnet flux switching generator for wind applications via artificial neural network and multi-objective particle swarm optimization hybrid approach. *Energy Conversion and Management, 110*, 230–239. https://doi.org/10.1016/j.enconman.2015.11.052
17. Rodriguez, J., et al. (2013). State of the art of finite control set model predictive control in power electronics. *IEEE Transactions on Industrial Informatics, 9*(2), 1003–1016. https://doi.org/10.1109/TII.2012.2207101
18. Islam, K. S., Shen, W., Mahmud, A., Chowdhury, M. A., & Zhang, J. (2016). Stability enhancement of DFIG wind turbine using LQR pitch control over rated wind speed. In *2016 IEEE 11th Conference on Industrial Electronics and Applications (ICIEA)* (pp. 1714–1719). IEEE. https://doi.org/10.1109/ICIEA.2016.7603834
19. Bhushan, R., & Chatterjee, K. (2017). Mathematical modeling and control of DFIG-based wind energy system by using optimized linear quadratic regulator weight matrices. *International Transactions on Electrical Energy Systems, 27*(11), e2377. https://doi.org/10.1002/etep.2377
20. Saad, N. H., Sattar, A. A., & Mansour, A. E. A. M. (2015). Low voltage ride through of doubly-fed induction generator connected to the grid using sliding mode control strategy. *Renewable Energy, 80*, 583–594. https://doi.org/10.1016/j.renene.2015.02.043
21. Han, Y., & Liu, X. (2016). Continuous higher-order sliding mode control with time-varying gain for a class of uncertain nonlinear systems. *ISA Transactions, 62*, 193–201. https://doi.org/10.1016/j.isatra.2016.01.014
22. Beltran, B., Benbouzid, M. E. H., & Ahmed-Ali, T. (2012). Second-order sliding mode control of a doubly fed induction generator driven wind turbine. *IEEE Transactions on Energy Conversion, 27*(2), 261–269. https://doi.org/10.1109/TEC.2011.2177092
23. Patnaik, R. K., & Dash, P. K. (2016). Fast adaptive back-stepping terminal sliding mode power control for both the rotor-side as well as grid-side converter of the doubly fed induction generator-based wind farms. *IET Renewable Power Generation, 10*(5), 598–610. https://doi.org/10.1049/iet-rpg.2015.0171
24. Shahgholian, G., & Izadpanahi, N. (2016). Improving the performance of wind turbine equipped with DFIG using STATCOM based on input-output feedback linearization controller. *Energy Equipment and Systems, 4*(1), 65–79. https://doi.org/10.22059/ees.2016.57945
25. Wu, F., Zhang, X., Ju, P., & Sterling, M. J. H. (2008). Decentralized nonlinear control of wind turbine with doubly fed induction generator. *IEEE Transactions on Power Systems, 23*(2), 613–621. https://doi.org/10.1109/TPWRS.2008.919421
26. Lin, X., Xiahou, K. S., Liu, Y., Zhang, Y. B., & Wu, Q. H. (2016). Maximum power point tracking of DFIG-WT using feedback linearization control based current regulators. In *2016 IEEE Innovative Smart Grid Technologies - Asia (ISGT-Asia)* (pp. 718–723). IEEE. https://doi.org/10.1109/ISGT-Asia.2016.7796419
27. Sleiman, M., Kedjar, B., Hamadi, A., Al-Haddad, K., & Kanaan, H. Y. (2013). Modeling, control and simulation of DFIG for maximum power point tracking. In *2013 9th Asian Control Conference (ASCC)* (pp. 1–6). IEEE. https://doi.org/10.1109/ASCC.2013.6606263

28. Abad, G., Lopez, J., Rodriguez, M. A., Marroyo, L., & Iwanski, G. (2011). *Doubly fed induction machine: Modeling and control for wind energy generation* (1st ed.). John Wiley & Sons.
29. Ljung, L. (1987). *System identification: Theory for the user*. Prentice Hall.
30. Mayne, D. Q., Rawlings, J. B., Rao, C. V., & Scokaert, P. O. M. (2000). Constrained model predictive control: Stability and optimality. *Automatica, 36*(6), 789–814. https://doi.org/10.1016/S0005-1098(99)00214-9
31. Wang, L. (2009). *Model predictive control system design and implementation using MATLAB*. Springer.
32. Sun, Y., Yan, S., Cai, B., & Wu, Y. (2018). Maximum power point tracking of DFIG with DC-based converter system using coordinated feedback linearization control. *Mathematical Problems in Engineering, 2018*, Article ID 9642123. https://doi.org/10.1155/2018/9642123
33. https://www.google.com/search?q=what+are+the+advantages+and+disadvantages+of+Feedback+Linearization+Based+Model+Predictive+control+of+Rotor+Speed+of+DFIGWT&oq=what+are+the+advantages+and+disadvantages+of+Feedback+Linearization+Based+Model+Predictive+control+of+Rotor+Speed+of+DFIGWT&gs_lcrp=EgZjaHJvbWUyBggAEEUYOTIHCAEQIRiPAtIBCjM0MjQ5ajBqMTWoAgiwAgHxBejMQihLqQUj8QXozEIoS6kFIw&sourceid=chrome&ie=UTF-8
34. Abdussamad, M. F., Abubakar, S. I., Nurudeen, D. G., Muhammad, M. H., & Muhammad, A. B. (2024). Feedback linearization-based model predictive control of rotor speed of DFIG-WT. *Global Journal of Research in Engineering & Computer Sciences, 4*(6), 95–106. https://doi.org/10.5281/zenodo.14488485

CITATION

Ahmed, S. A., Isah, A. L., Kabir, A., Mohammed, M. D., Ahmad, A. M., & Said, M. A. (2025). Repercussions and Difficulties of Feedback Linearization-Based Optimal Control of a DoublyFed Induction Generator. In Global Journal of Research in Engineering & Computer Sciences (Vol. 5, Number 4, pp. 26–38). https://doi.org/10.5281/zenodo.16739653